

RESEARCH REPORT

STEM CELLS AND REGENERATION

Characterisation of the human embryonic and foetal epicardium during heart development

Catherine A. Risebro^{1,*}, Joaquim Miguel Vieira^{2,*}, Linda Klotz¹ and Paul R. Riley^{1,2,‡}

ABSTRACT

The epicardium is essential for mammalian heart development. At present, our understanding of the timing and morphogenetic events leading to the formation of the human epicardium has essentially been extrapolated from model organisms. Here, we studied primary tissue samples to characterise human epicardium development. We reveal that the epicardium begins to envelop the myocardial surface at Carnegie stage (CS) 11 and this process is completed by CS15, earlier than previously inferred from avian studies. Contrary to prevailing dogma, the formed human epicardium is not a simple squamous epithelium and we reveal evidence of more complex structure, including novel spatial differences aligned to the developing chambers. Specifically, the ventricular, but not atrial, epicardium exhibited areas of expanded epithelium, preferential cell alignment and spindle-like morphology. Likewise, we reveal distinct properties *ex vivo*, such that ventricular cells spontaneously differentiate and lose epicardial identity, whereas atrial-derived cells remained 'epithelial-like'. These data provide insight into the developing human epicardium that may contribute to our understanding of congenital heart disease and have implications for the development of strategies for endogenous cell-based cardiac repair.

KEY WORDS: Human, Heart, Epicardium, Regeneration, Epithelial-to-mesenchymal transition

INTRODUCTION

Congenital heart defects (CHDs) affect 1–2% of newborn children and are the leading cause of death in infants under 1 year of age. Despite their prevalence, the aetiology of many CHDs remains unknown. Experimental animal studies have contributed substantially to our understanding of normal and abnormal heart development; however, there is a pre-clinical need to study the ontology of the human foetal heart and to accurately map morphogenetic and cellular defects that might underpin congenital heart disease. Beyond an application to birth defects, characterisation of the events orchestrating heart development has emerged as a paradigm to identify cellular sources for repair of the injured adult heart (Smart et al., 2007, 2011; Zhou et al., 2011). The epicardium and epicardium-derived cells (EPDCs) are essential for normal heart development, as studied in animal models, and contribute fibroblasts and coronary smooth muscle to the growing heart. Additional contributions to coronary endothelium and cardiomyocytes have also been revealed; however, the full extent

to which epicardium acts as a source of these lineages is controversial (Cai et al., 2008; Dettman et al., 1998; Katz et al., 2012; Zhou et al., 2008). Further to cell contribution, epicardium-derived factors (e.g. retinoic acid) regulate cardiomyocyte proliferation and the growth of developing chamber myocardium (Pérez-Pomares et al., 2002). In turn, myocardial growth factors (e.g. fibroblast growth factors, thymosin beta 4) regulate EPDC fate by promoting epithelial-to-mesenchymal transition (EMT), invasion of the subepicardial space and subsequent cell differentiation (Cai et al., 2008; Morabito et al., 2001; Pérez-Pomares et al., 2002; Smart et al., 2007). As a result, reciprocal signalling between the epicardium and underlying myocardium is essential (Schlueter and Brand, 2012) and, if impaired, results in a broad spectrum of CHDs, including abnormal coronary vasculogenesis and ventricular non-compaction (Merki et al., 2005).

The epicardium arises from the proepicardium (PE), a mesoderm-derived transitory structure that develops at the base of the inflow tract in all vertebrate hearts [e.g. 60 h of incubation in the chicken embryo; embryonic days (E) 9.0–9.5 in the mouse embryo; fourth week post-conception in the human embryo] (Ruiz-Villalba and Perez-Pomares, 2012). PE-derived cells are transferred across the fluid-rich pericardial cavity and, upon attachment onto the outer surface of the early embryonic heart, migrate and expand to form a single-layered flat epithelium (epicardium) connected to the myocardium by subepicardial tissue (Manner et al., 2001). The latter events have been unequivocally clarified by electron microscopy in representative vertebrate species, including *Gallus gallus* (chicken), *Danio rerio* (zebrafish) and *Mus musculus* (mouse) as previously reviewed (Schlueter and Brand, 2012). Yet, characterisation of human epicardial development remains ill-defined, largely owing to the challenges of accessing foetal heart tissue and the limitations in the experimental approaches that can be applied to human studies. Indeed, to the best of our knowledge only one prior study offers a rudimentary insight into epicardial formation in humans (Hirakow, 1992). Light microscopy imaging of serial histological sections from staged human embryos at Carnegie stages (CS) 12 to 17 (4–6 weeks post-conception; equivalent to E9.5–12.5 in the mouse embryo) was employed to infer that morphogenetic events analogous to those described in the chicken embryo governed initial epicardial formation at CS12 (Hirakow, 1992; Manner et al., 2001). Villous protrusions of PE-derived cells extending from the sinus wall region contacted the ventricle on the dorsal side and then spread out as a single squamous epithelium (Hirakow, 1992; Manner et al., 2001; Sylva et al., 2014). Despite these early anatomical descriptions, virtually nothing is known about the cellular architecture, marker expression and lineage potential of the human embryonic epicardium across later stages of heart development.

In the present study, we made use of three-dimensional (3D) optical projection tomography (OPT), confocal laser scanning

¹UCL-Institute of Child Health, Molecular Medicine Unit, 30 Guilford Street, London WC1N 1EH, UK. ²University of Oxford, Department of Physiology, Anatomy and Genetics, South Parks Road, Oxford OX1 3PT, UK.

*These authors contributed equally to this work

†Author for correspondence (paul.riley@dpag.ox.ac.uk)

Received 17 June 2015; Accepted 8 September 2015

microscopy and *ex vivo* epicardial cultures to characterise the human epicardium from embryonic stage CS11 to foetal stage (F) 3, i.e. between 4 and 11 weeks post-conception. The human material was obtained from the MRC-Wellcome Trust Human Development Biology Resource (HDBR) (Lindsay and Copp, 2005). Our findings revealed initiation of human epicardial development at CS11 (equivalent to E8.5–9.0 in the mouse embryo) and completion of epithelium formation by CS15. We observed expression of markers previously reported in the developing epicardium of other vertebrate species, including WT1, TCF21, GATA5, TBX18, cytokeratins and podoplanin, and highlighted novel differences between the atrial and ventricular epicardium. Significant chamber differences both in terms of overlying epicardial structure and EPDC-differentiation potential *ex vivo* were evident, which might underlie a heterogeneous contribution during development and regional contributions to phenotypes underlying human birth defects.

RESULTS AND DISCUSSION

The epicardium covers the entire human embryonic heart between CS14 and CS15

Previous observations have suggested that epicardial growth starts by CS12 (4 weeks post-conception; equivalent to E9.5 in mouse embryos), a time point coinciding with looping of the human embryonic heart (Hirakow, 1992; Sylva et al., 2014). To further characterise the development of the embryonic epicardium, we analysed Haematoxylin and Eosin-stained serial sections of paraffin-embedded human hearts at stages CS11 to CS14 (between 4 and 5 weeks post-conception; $n=3$ per stage; Fig. S1; data not shown). At CS11, some cells were already observed covering small extensions of the developing compact myocardial layer; however, these cells were round and progenitor-like (high nuclear-cytoplasmic ratios) and lacked the stereotypical thin and flat (squamous) epithelial morphology (Fig. S1A–C). Between CS12 and CS14, the outer layer of the embryonic heart became squamous-like and expanded to cover most of the developing ventricle and atrial myocardium (Fig. S1D–F, arrowheads; data not shown). Importantly, this is earlier than previously described; based exclusively on extrapolating from findings in the chicken embryonic heart, it was previously suggested that the epicardium covers the entire heart by late stage CS16 (Hirakow, 1992; Sylva et al., 2014).

To provide insight into the developing human epicardium in the context of the overall changes in heart morphology, we initially performed OPT at a resolution of 5–10 µm with 3D-volume rendering (Fig. 1A–H) to observe the gross anatomy and patterning of the heart (Norris et al., 2013; Ruijter et al., 2004). At late stage CS15 (5 weeks post-conception; equivalent to E11.0 in the mouse embryo; $n=2$; Fig. 1A,B), CS18 (7 weeks post-conception; equivalent to E12.5 in the mouse embryo; $n=2$; Fig. 1C,D), CS20 (8 weeks post-conception; equivalent to E13.5 in the mouse embryo; $n=2$; Fig. 1E,F) and CS23 (8 weeks post-conception; equivalent to E14.5 in the mouse embryo; $n=2$; Fig. 1G,H) autofluorescence and OPT revealed the progression of heart development with radial and apical expansion, leading to the stereotypical four-chamber shaped heart by CS23. Histological analyses of human hearts post-OPT imaging confirmed full epicardial coverage of the underlying myocardium with the formation of an intact epithelium by CS15 (Fig. 1I–L; data not shown). To establish the epicardial identity of this forming (outer) epithelial layer, we performed immunostaining of sections along the short (transverse) and long (apical-basal) axis of hearts at CS13 to

CS18 (4–7 weeks post-conception; equivalent to E11.0–12.5 in the mouse embryo) using an antibody specific for the transcription factor WT1 (Fig. 1M–R; Fig. S2A–K). At CS13, WT1-expressing cells were observed (Fig. S2A–F), which between CS14 and CS15 expanded to give rise to an outer WT1-positive layer enveloping the developing myocardium (Fig. S2G–K and Fig. 1M–O, respectively). At CS18, the entire epicardium exhibited nuclear expression of WT1 (Fig. 1P–R). Taken together, our observations suggest that epicardial growth initiates and completes earlier than previously anticipated.

The human ventricular, but not atrial, epicardium forms as a multiple-cell layered epithelium

To further characterise the human embryonic epicardium, we extended the immunostaining studies to include sections through the long axis of hearts at CS20 and CS23 (8 weeks post-conception; equivalent to E13.5 and E14.5 in the mouse embryo, respectively) and used antibodies specific for WT1 and additional markers (Fig. 2; Fig. S3), including the transcription factor TCF21, the surface glycoprotein podoplanin, which also labels the lymphatic endothelium and cytokeratins, components of the intermediate filaments of the cytoskeleton within epithelia that have been shown to label the developing epicardium (Braitsch et al., 2013; Smart et al., 2011; Vrancken Peeters et al., 1995). Significantly, podoplanin-positive (Fig. 2A) cells residing on the outer surface of the embryonic heart were also positive for TCF21 (Fig. 2B) and WT1 expression (Fig. 2C) at CS20. However, whereas the atrial epicardium represented a uniform podoplanin- and WT1-expressing single-cell layer (Fig. 2D–G), areas of expanded epicardium were observed in the ventricles (Fig. 2H–K), demarcated by podoplanin expression (Fig. 2J, double-arrow) and comprising several WT1-positive cell layers (Fig. 2K, double-arrow). Similar observations were made in sections from embryonic hearts at late stage CS23 (Fig. 2L–S; Fig. S3I–P). Moreover, close examination of sections from embryonic hearts at CS17 (6 weeks post-conception; equivalent to E12.0–12.5 in the mouse embryo) revealed areas of expanded epicardium in the ventricles already at this early stage of development (Fig. S3E–H).

The expanded epicardium in the ventricles exhibited strong expression of canonical EMT markers (Fig. S3I–V), including the activating transcription factor ZEB1 and the induced mesenchymal marker vimentin (Kim et al., 2014). This is consistent with animal studies in which EMT underpins the migration of EPDCs into the subepicardial layer, prior to contributing derivatives to the developing coronary arteries and interstitial fibroblasts (Sylva et al., 2014). Areas of thickened epicardium were still detected overlying the ventricular, but not atrial, surface (Fig. S4, arrowheads) of hearts at foetal stage F3 (11 weeks post-conception; equivalent to E17.5–18.5 in the mouse embryo). This data highlights previously unappreciated differences between human atrial and ventricular epicardium: contrary to the predominant view of the epicardium as a uniform single layer of squamous epithelium covering the myocardium, the human ventricular epicardium contains regions of multiple cell layers, which persist in the foetal heart after subepicardial mesenchyme induction and EPDC differentiation into different cardiovascular cell types.

Human ventricular and atrial epicardium exhibit different cytokeratin expression patterns and cell-cell arrangements

To investigate further potential differences between the atrial and ventricular human epicardium, we performed whole-mount staining

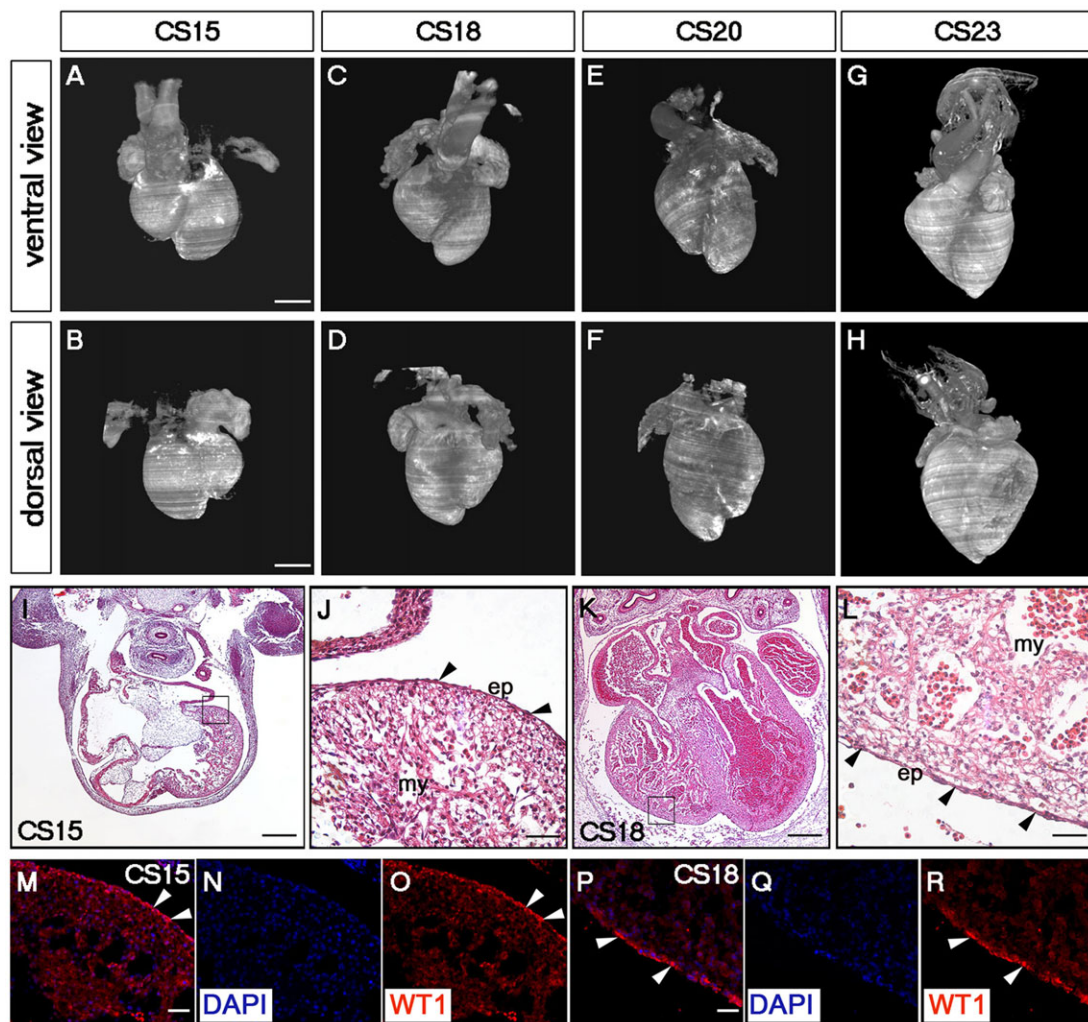


Fig. 1. The human embryonic epicardium completely covers the developing myocardium by CS15. (A–H) Ventral and dorsal views of 3D OPT-based reconstructions of heart specimens at CS15, CS18, CS20 and CS23. (I–L) Haematoxylin and Eosin-stained coronal sections of human specimens at CS15 and CS18. Arrowheads (J,L) indicate the flat single-cell squamous epithelium covering the developing myocardium. (M–R) Confocal imaging of sections along the apical-basal axis of embryonic hearts at CS15 (M–O) and CS18 (P–R) immunostained with the epicardial marker WT1. Arrowheads (M,O,P,R) indicate WT1-positive epicardial cells. ep, epicardium; my, myocardium. Scale bars: 1 mm (A–H); 200 µm (I,K); 25 µm (J,L); 20 µm (M,P).

for WT1 and cytokeratin (Fig. 3). Antibodies against cytokeratins have been used to visualise the migrating pattern of epicardial cells in the whole-mount quail heart, allowing insight into some of the morphological events associated with avian epicardium formation (Vrancken Peeters et al., 1995). At CS17 (6 weeks post-conception; equivalent to E12.0–12.5 in the mouse embryo), cytokeratin expression was widespread throughout the embryonic epicardium and colocalised with WT1 (Fig. 3A–E). Although no obvious differences in the pattern of cytokeratin expression were observed between the atrial and ventricular epicardium at CS17, regional differences were apparent at late foetal stage F2 (10 weeks post-conception; equivalent to E16.5–17.5 in the mouse embryo). Cytokeratin/WT1 double-positive epicardial cells were distributed in a stochastic fashion on the atrial surface with diffuse cytokeratin expression throughout the cytoplasm, whereas the ventricular epicardial cells exhibited a spindle-cell morphology and preferential alignment, being orientated side-by-side with strong cytokeratin staining outlining the cell membrane and cytoskeletal filaments (compare Fig. 3F–H with 3I–K). These observations suggest that during foetal heart development the human ventricular epicardium conforms to a more polarised and differentiated

epithelium, whereas the atrial epicardium retains an embryonic-like morphology.

Human ventricular, but not atrial EPDCs spontaneously undergo EMT ex vivo

To investigate whether the differences in epicardium formation between the chambers underlie distinct potential and capacity for differentiation, we performed *ex vivo* cultures of epicardium dissected from the atria and ventricles of human hearts at CS17 and CS23 (Fig. 4), i.e. 6 and 8 weeks post-conception (equivalent to E12.0–12.5 and E14.5 in the mouse embryo, respectively). Both atrial and ventricular explants resulted in the outgrowth of cells after 48 h in culture (Fig. 4A–D). However, atrial EPDCs exhibited an epithelial cobblestone-like morphology (Fig. 4A,C), whereas primary ventricular EPDCs predominantly outgrew with a spindle-like mesenchymal morphology (Fig. 4B,D). Furthermore, the atrial outgrowths displayed robust nuclear WT1, TCF21, GATA5 and TBX18 staining (Fig. 4E–H) confirming their epicardial identity, whereas the ventricular equivalent exhibited reduced nuclear WT1, cytoplasmic TCF21 and perinuclear GATA5 and TBX18 staining (Fig. 4I–L). These observations suggested that primary cells derived

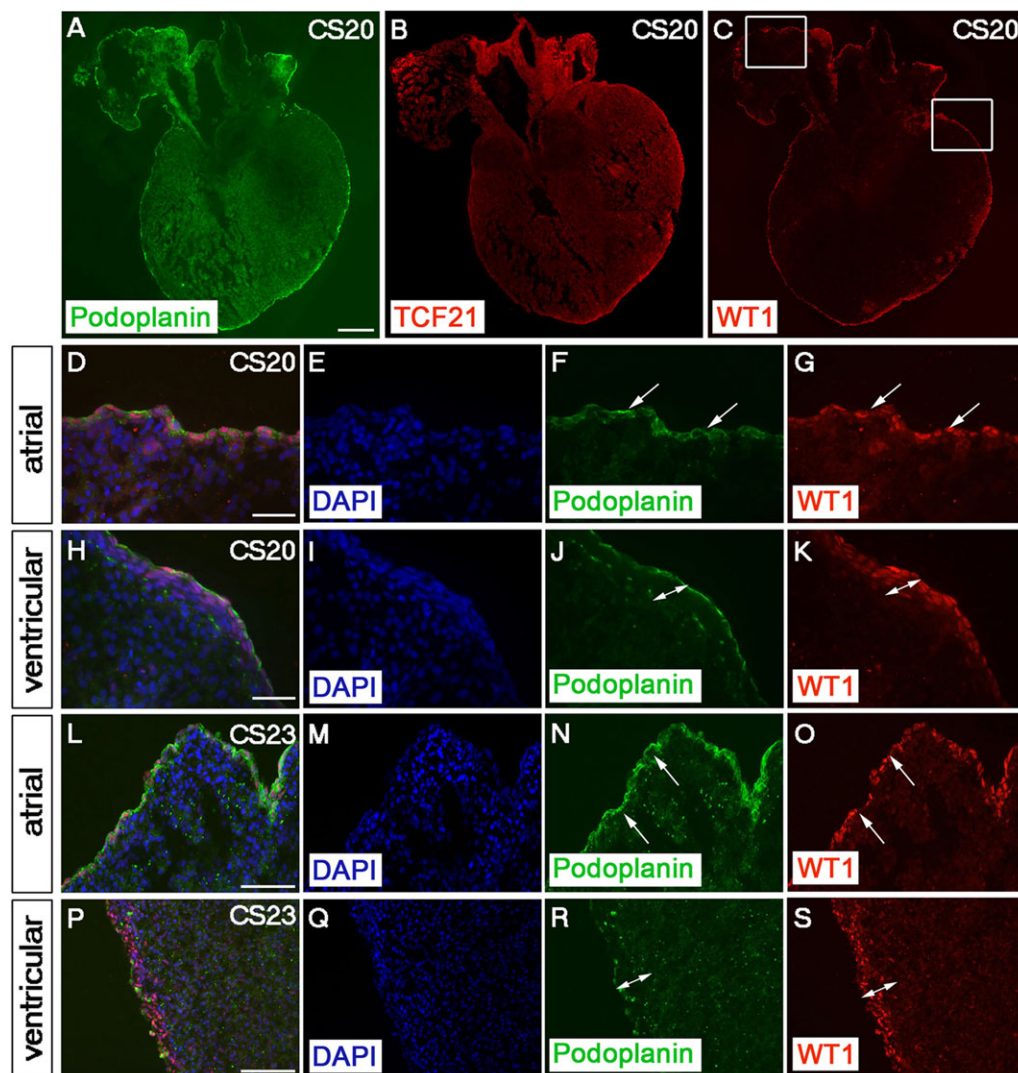


Fig. 2. The ventricular, but not atrial, epicardium of the embryonic human heart comprises areas of expanded epithelium.

(A–K) Confocal imaging of sections along the apical–basal axis of embryonic hearts at CS20 immunostained with the epicardial markers podoplanin, TCF21 and WT1 (boxed area in the atrium is enlarged in D–G; boxed area in the ventricle is enlarged in H–K).

(L–S) Confocal imaging of sections of embryonic hearts at CS23 immunostained with the epicardial markers podoplanin and WT1. White arrows in F,G,N,O indicate the atrial single-cell layer. White double-arrows in J,K,R,S indicate the expanded ventricular epicardium. Scale bars: 200 µm (A–C); 40 µm (D–K); 100 µm (L–S).

from the ventricular epicardium spontaneously undergo EMT. In support of this hypothesis, (nuclear) WT1-expressing atrial EPDCs exhibited membrane alpha-smooth muscle actin (α SMA) staining, demarcating their epithelial cell shape (Fig. 4M,N), whereas primary ventricular EPDCs displayed intense cytoplasmic α SMA staining (Fig. 4O,P), labelling the filamentous actin cytoskeleton, a characteristic feature of smooth muscle cells and myofibroblasts (Willems et al., 1994).

Conclusions

The study of human embryonic and foetal hearts to understand normal heart development validates and extends prior animal model studies and serves to advance our understanding of human anatomical birth defects that underpin congenital heart disease. The human material utilised herein had a normal karyotype; however, the HDBR banks chromosomally abnormal material, which may enable studies on other genetic backgrounds to further dissect the impact of abnormal heart development. In this study, we focused exclusively on the epicardium, given that in animal studies it contributes to the major cardiovascular cell types and plays essential roles in regulating the development of the coronaries and growth of the myocardium, both of which are substrates for cohorts of CHD, including hypoplastic left heart and ventricular non-compaction.

Our findings challenge the idea of the human epicardium forming as a single-cell layer of squamous epithelium covering the outer surface of the heart as would be inferred from model organisms. We reveal that the embryonic and foetal epicardium enveloping the ventricles, but not atria, of the human heart comprises areas of thickened epithelium proximal to blood vessels, which resemble the tertiary structures previously described in the post-natal murine heart (Balmer et al., 2014). These structures in mouse assembled during the so-called neonatal regenerative window (P1–P7) (Porrello et al., 2011) as extracellular matrix (ECM)-encased clusters containing haematopoietic cells and further responded to myocardial injury in the adult setting by proliferating, releasing cells and re-encapsulating post-injury. Therefore, we suggest similar tertiary structures might assemble in the developing epicardium of the human heart, and it will be of interest to characterise further their cellular and matrix components, and investigate whether these structures are transient or persist through to adult stages.

Our study raises the issue of fundamental differences in the architecture of atrial and ventricular epicardium, established during human heart development. This does not appear to have been addressed in animal models to date, and suggests that the epicardium is a heterogeneous lineage, not only defined by its cellular composition (as described in the mouse) (Balmer et al., 2014) but also by regional subsets of epicardial cells that may

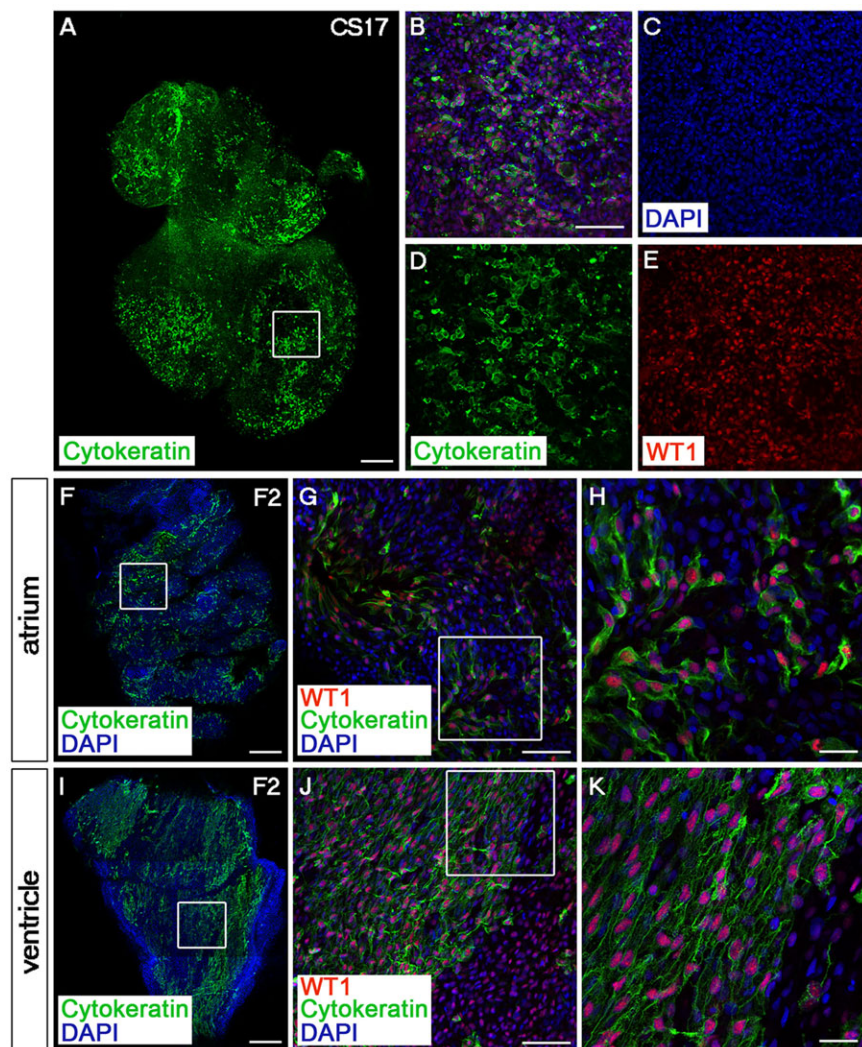


Fig. 3. The developing atrial and ventricular epicardium exhibit different cytokeratin expression patterns and cellular alignment. (A-E) Whole-mount confocal imaging of human hearts at embryonic stage CS17 immunostained with the epicardial markers cytokeratin and WT1 (boxed area in A is enlarged in B-E). (F-H) Whole-mount confocal imaging of the human atrium at foetal stage F2 immunostained with cytokeratin and WT1 (boxed area in F is enlarged in G; boxed area in G is enlarged in H). (I-K) Whole-mount confocal imaging of a human ventricle at foetal stage F2 immunostained with cytokeratin and WT1 (boxed area in I is enlarged in J; boxed area in J is enlarged in K). Scale bars: 100 µm (A-G,I,J); 40 µm (H,K).

underlie spatial differences in EPDC potential. We reveal that the ventricular epicardium of the foetal human heart is polarised, in contrast to the atrial lineage, and exhibits a spindle-like morphology that, when cultured *ex vivo*, spontaneously adopts a differentiated phenotype and loses its epicardial identity. This is relevant beyond heart development in that, previously, epicardium derived from right atrial appendages of human patients has been cultured *ex vivo* with primary EPDCs undergoing EMT in response to TGF β and differentiating into smooth muscle cells (van Tuyn et al., 2007). The same primary cells administered to a murine model of myocardial injury (MI) ameliorated cardiac function, reinforcing the hypothesis that EPDCs could be a suitable cell source for cardiac cell therapy (Winter et al., 2007). Given the differences we observe between embryonic ventricular and atrial epicardium herein, a priority moving forward would be to determine the regenerative potential of the adult ventricular lineage in the context of ischaemic disease.

MATERIALS AND METHODS

Human tissue

Hearts were dissected from human foetal and embryonic terminations of pregnancies obtained from the MRC-Wellcome Trust Human Developmental Biology Resource (HDBR) at UCL Institute of Child Health. Tissue from ages between 4 and 11 weeks post-conception (CS11-F3, total $n=37$; CS11, $n=3$; CS13, $n=3$; CS14, $n=3$; CS15, $n=3$; CS17, $n=5$; CS18, $n=2$; CS20, $n=4$; CS23, $n=7$; F2, $n=4$; F3, $n=3$) was used for OPT,

histology, immunostaining or *ex vivo* epicardial culture. All tissues were used with maternal consent and approval of the Institute of Human Genetics, Newcastle and UCL Institute of Child Health Ethics Committee. Age was estimated from measurements of foot length and heel to knee length and compared with a standard growth chart (Hern, 1984).

Ex vivo culture of human embryonic EPDCs

EPDCs were cultured from embryonic atrial and ventricular epicardium stripped from hearts at CS17 and CS23 (7–8 weeks post-conception). The stripped layer of epicardium was placed in a 35-mm culture dish (Corning Costar) coated with 0.1% porcine gelatine solution (weight/volume in PBS; both Sigma) and topped with an 18Mmedium (DMEM) and medium 199 (M199) containing 100 U/ml penicillin, 100 µg/ml streptomycin, 10% foetal bovine serum (FBS; Invitrogen). The culture medium was refreshed every 2 days. Once epithelium-like cell outgrowth was visible (on average 48 h after initiation of the culture), EPDCs were either detached with trypsin (Invitrogen) to establish subcultures or processed for immunostaining using the antibodies described below. Characterisation of atrial and ventricular EPDCs was performed with at least three independent *ex vivo* cultures per embryonic stage.

Histology

For histology, specimens were fixed in 4% formaldehyde, dehydrated and paraffin-embedded (Raymond Lamb) in plastic moulds and left to set overnight at room temperature. Paraffin blocks were sectioned using a Microm HM325 microtome and 10 µm sections stained with Haematoxylin and Eosin (both Sigma). Sections were imaged using a Zeiss SteREO

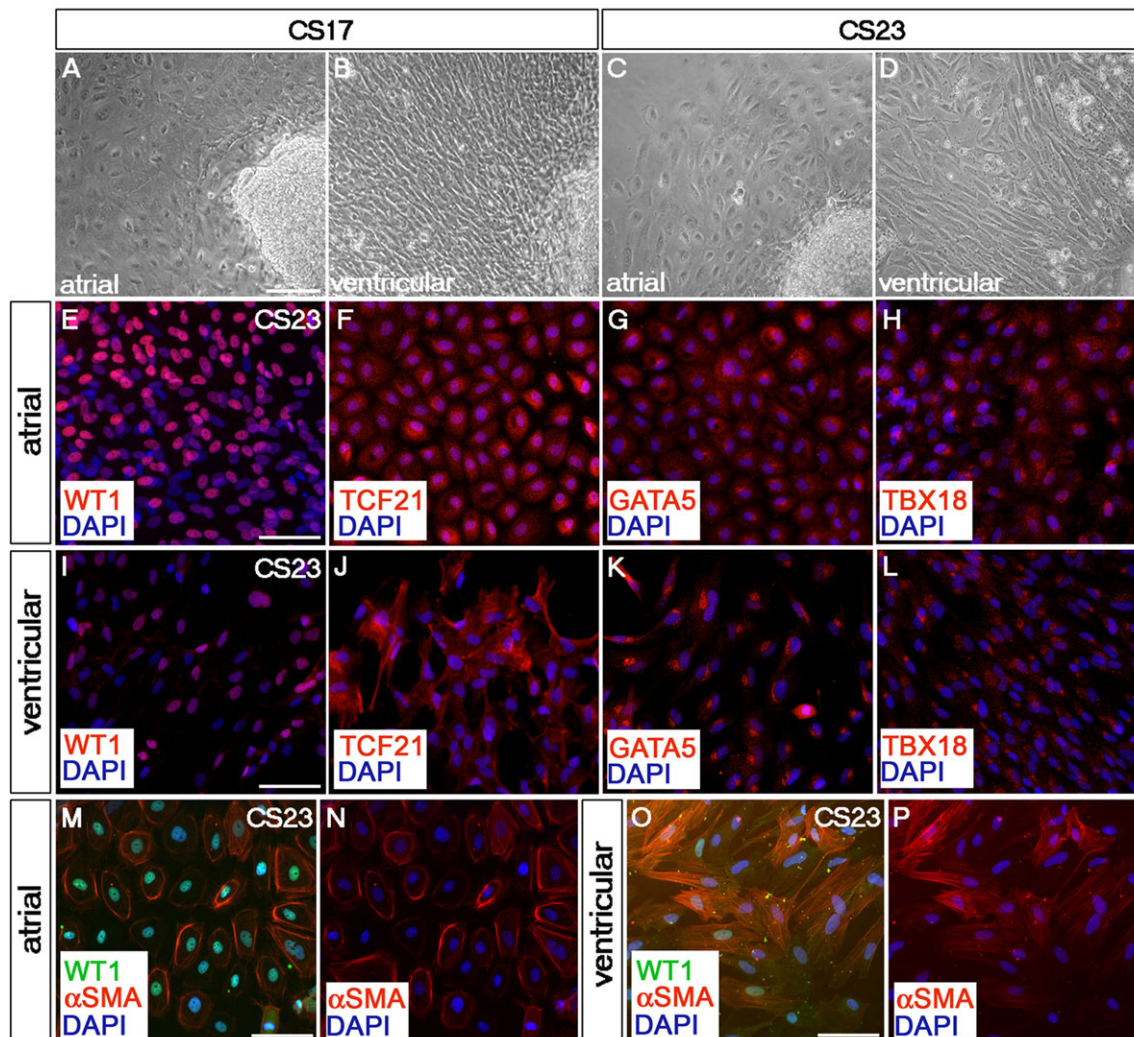


Fig. 4. Primary epicardial cells derived from the atrial epicardium exhibit an epitheloid cobblestone-like morphology, whereas cells derived from ventricular epicardium spontaneously differentiate ex vivo. (A–D) Bright-field imaging of embryonic epicardial explants derived from the atria (A,C) or ventricles (B,D) of human hearts at CS17 (A,B) and CS23 (C,D) cultured ex vivo for 48 h. (E–L) Imaging of atrial-derived (E–H) or ventricular-derived (I–L) EPDCs immunostained with the epicardial markers WT1, TCF21, GATA5 and TBX18. (M–P) Imaging of atrial-derived (M,N) or ventricular-derived (O,P) EPDCs immunostained with the markers αSMA and WT1. Scale bars: 100 µm.

Luma2.V2 stereo microscope with a Zeiss HRc AxioCam attachment and AxioVision software release 4.8 (all Carl Zeiss).

Immunostaining

Heart samples were fixed in 4% formaldehyde and processed for indirect immunofluorescence using either standard whole-mount or cryosection staining methods. Primary antibodies used were: monoclonal mouse anti-human cytokeratin (Dako, clone MNF116, 1:100), monoclonal mouse anti-podoplanin (Abcam, clone D2-40, 1:40), mouse monoclonal anti-smooth muscle cell (SMC) α-actin (Sigma, clone 1A4, 1:100), rabbit monoclonal anti-WT1 [Abcam, clone CAN-R9(IHC)-56-2, 1:200], rabbit monoclonal anti-Vimentin (Abcam, clone EPR3776, 1:100), rabbit polyclonal anti-TBX18 (Abcam, ab51397, 1:350), rabbit polyclonal anti-TCF21 (Abcam, ab32981, 1:100), rabbit polyclonal anti-GATA5 (Abcam, ab48820, 1:100), rabbit polyclonal anti-ZEB1 (kind gift from Prof Xin Lu, Ludwig Cancer Research, Oxford, UK; 1:100). AlexaFluor-conjugated secondary antibodies (Life Technologies, 1:200) were used in all cases. Imaging was performed using a Zeiss LSM710 confocal microscope (whole-mount), using the 405, 488, 561 and 647 nm lasers and Zen software (Carl Zeiss), or a Zeiss Axio Imager Z1 microscope (cryosections) with an AxioCam MRm camera attachment running AxioVision software release 4.8 (Carl Zeiss). Image processing analysis

was performed using Fiji software. All confocal images are maximum intensity projections of z-stacks.

Optical projection tomography (OPT) scanning

Heart samples were fixed in 4% formaldehyde, washed repeatedly in distilled water and embedded in 1% ultrapure low melting point agarose (Life Technologies) solution. Agarose blocks were cut into a pyramidal octagon around the tissue sample and dehydrated in two overnight washes in 100% methanol, before undergoing two to three overnight washes in 2:1 benzyl aminobenzoate-benzyl alcohol (BABB; both Sigma) solution for clearing. The agarose pyramid was then glued to an OPT mount (Bioptonics). Scanning was performed on a Bioptronics machine using the SkyScan3001 software. Samples were centred prior to scanning and put in focus on each of the channels (GFP+ for Alexa488, TXR for Alexa647). All samples were scanned at high resolution in a 360° rotation with intervals of 0.45°. Images were processed using the NRecon and Fiji software.

Acknowledgements

The human embryonic and foetal material was provided by the Joint MRC-Wellcome Trust (grant # 099175/Z/12/Z) Human Developmental Biology Resource (<http://www.hdbi.org>) at the UCL Institute of Child Health. We are grateful to Xin Lu for providing reagents and Bertrand Vernay for assistance with optical projection

tomography scanning and data processing. We thank Chia Yeo and Anke Smits for helping with tissue collection.

Competing interests

The authors declare no competing or financial interests.

Author contributions

C.A.R., J.M.V. and P.R.R. designed the study. C.A.R., L.K. and J.M.V. performed the experiments and analysed the data. J.M.V. and P.R.R. wrote the manuscript. All authors have read, commented on and approved the manuscript.

Funding

This work was supported by the British Heart Foundation [programme grant RG/08/003/25264 to J.V. and P.R.R.; project grant PG/09/043/27565 to C.A.R.] and the Wellcome Trust [PhD Studentship 083345 to L.K.]. Deposited in PMC for release after 6 months.

Supplementary information

Supplementary information available online at
<http://dev.biologists.org/lookup/suppl/doi:10.1242/dev.127621/-DC1>

References

- Balmer, G. M., Bollini, S., Dubé, K. N., Martinez-Barbera, J. P., Williams, O. and Riley, P. R. (2014). Dynamic haematopoietic cell contribution to the developing and adult epicardium. *Nat. Commun.* **5**, 4054.
- Braitsch, C. M., Kanisicka, O., van Berlo, J. H., Molkenkin, J. D. and Yutzey, K. E. (2013). Differential expression of embryonic epicardial progenitor markers and localization of cardiac fibrosis in adult ischemic injury and hypertensive heart disease. *J. Mol. Cell. Cardiol.* **65**, 108-119.
- Cai, C.-L., Martin, J. C., Sun, Y., Cui, L., Wang, L., Ouyang, K., Yang, L., Bu, L., Liang, X., Zhang, X. et al. (2008). A myocardial lineage derives from Tbx18 epicardial cells. *Nature* **454**, 104-108.
- Dettman, R. W., Denetclaw, W., Jr, Ordahl, C. P. and Bristow, J. (1998). Common epicardial origin of coronary vascular smooth muscle, perivascular fibroblasts, and intermyocardial fibroblasts in the avian heart. *Dev. Biol.* **193**, 169-181.
- Hern, W. M. (1984). Correlation of fetal age and measurements between 10 and 26 weeks of gestation. *Obstet. Gynecol.* **63**, 26-32.
- Hirakow, R. (1992). Epicardial formation in staged human embryos. *Kaibogaku Zasshi* **67**, 616-622.
- Katz, T. C., Singh, M. K., Degenhardt, K., Rivera-Feliciano, J., Johnson, R. L., Epstein, J. A. and Tabin, C. J. (2012). Distinct compartments of the proepicardial organ give rise to coronary vascular endothelial cells. *Dev. Cell* **22**, 639-650.
- Kim, Y.-S., Yi, B.-R., Kim, N.-H. and Choi, K.-C. (2014). Role of the epithelial-mesenchymal transition and its effects on embryonic stem cells. *Exp. Mol. Med.* **46**, e108.
- Lindsay, S. and Copp, A. J. (2005). MRC-Wellcome Trust Human Developmental Biology Resource: enabling studies of human developmental gene expression. *Trends Genet.* **21**, 586-590.
- Männer, J., Pérez-Pomares, J. M., Macías, D. and Muñoz-Chápuli, R. (2001). The origin, formation and developmental significance of the epicardium: a review. *Cells Tissues Organs* **169**, 89-103.
- Merki, E., Zamora, M., Raya, A., Kawakami, Y., Wang, J., Zhang, X., Burch, J., Kubalak, S. W., Kaliman, P., Belmonte, J. C. I. et al. (2005). Epicardial retinoid X receptor alpha is required for myocardial growth and coronary artery formation. *Proc. Natl. Acad. Sci. USA* **102**, 18455-18460.
- Morabito, C. J., Dettman, R. W., Kattan, J., Collier, J. M. and Bristow, J. (2001). Positive and negative regulation of epicardial-mesenchymal transformation during avian heart development. *Dev. Biol.* **234**, 204-215.
- Norris, F. C., Wong, M. D., Greene, N. D. E., Scambler, P. J., Weaver, T., Weninger, W. J., Mohun, T. J., Henkelman, R. M. and Lythgoe, M. F. (2013). A coming of age: advanced imaging technologies for characterising the developing mouse. *Trends Genet.* **29**, 700-711.
- Pérez-Pomares, J. M., Phelps, A., Sedmerova, M., Carmona, R., González-Iriarte, M., Muñoz-Chápuli, R. and Wessels, A. (2002). Experimental studies on the spatiotemporal expression of WT1 and RALDH2 in the embryonic avian heart: a model for the regulation of myocardial and valvuloseptal development by epicardially derived cells (EPDCs). *Dev. Biol.* **247**, 307-326.
- Porrello, E. R., Mahmoud, A. I., Simpson, E., Hill, J. A., Richardson, J. A., Olson, E. N. and Sadek, H. A. (2011). Transient regenerative potential of the neonatal mouse heart. *Science* **331**, 1078-1080.
- Ruijter, J. M., Soufan, A. T., Hagoort, J. and Moorman, A. F. M. (2004). Molecular imaging of the embryonic heart: fables and facts on 3D imaging of gene expression patterns. *Birth Defects Res. C Embryo. Today Rev.* **72**, 224-240.
- Ruiz-Villalba, A. and Pérez-Pomares, J. M. (2012). The expanding role of the epicardium and epicardial-derived cells in cardiac development and disease. *Curr. Opin. Pediatr.* **24**, 569-576.
- Schlüter, J. and Brand, T. (2012). Epicardial progenitor cells in cardiac development and regeneration. *J. Cardiovasc. Transl. Res.* **5**, 641-653.
- Smart, N., Risebro, C. A., Melville, A. A. D., Moses, K., Schwartz, R. J., Chien, K. R. and Riley, P. R. (2007). Thymosin beta4 induces adult epicardial progenitor mobilization and neovascularization. *Nature* **445**, 177-182.
- Smart, N., Bollini, S., Dubé, K. N., Vieira, J. M., Zhou, B., Davidson, S., Yellon, D., Riegler, J., Price, A. N., Lythgoe, M. F. et al. (2011). De novo cardiomyocytes from within the activated adult heart after injury. *Nature* **474**, 640-644.
- Sylva, M., van den Hoff, M. J. B. and Moorman, A. F. M. (2014). Development of the human heart. *Am. J. Med. Genet. A* **164**, 1347-1371.
- van Tuyn, J., Atsma, D. E., Winter, E. M., van der Velde-van Dijke, I., Pijnappels, D. A., Bax, N. A. M., Knaän-Shanzer, S., Gittenberger-de Groot, A. C., Poelmann, R. E., van der Laarse, A. et al. (2007). Epicardial cells of human adults can undergo an epithelial-to-mesenchymal transition and obtain characteristics of smooth muscle cells in vitro. *Stem Cells* **25**, 271-278.
- Vrancken Peeters, M.-P. F. M., Mentink, M. M. T., Poelmann, R. E. and Gittenberger-de Groot, A. C. (1995). Cytokeratins as a marker for epicardial formation in the quail embryo. *Anat. Embryol.* **191**, 503-508.
- Willems, I. E., Havenith, M. G., De Mey, J. G. and Daemen, M. J. (1994). The alpha-smooth muscle actin-positive cells in healing human myocardial scars. *Am. J. Pathol.* **145**, 868-875.
- Winter, E. M., Grauss, R. W., Hogers, B., van Tuyn, J., van der Geest, R., Lie-Venema, H., Steijn, R. V., Maas, S., DeRuiter, M. C., deVries, A. A. F. et al. (2007). Preservation of left ventricular function and attenuation of remodeling after transplantation of human epicardium-derived cells into the infarcted mouse heart. *Circulation* **116**, 917-927.
- Zhou, B., Ma, Q., Rajagopal, S., Wu, S. M., Domian, I., Rivera-Feliciano, J., Jiang, D., von Gise, A., Ikeda, S., Chien, K. R. et al. (2008). Epicardial progenitors contribute to the cardiomyocyte lineage in the developing heart. *Nature* **454**, 109-113.
- Zhou, B., Honor, L. B., He, H., Ma, Q., Oh, J.-H., Butterfield, C., Lin, R.-Z., Melero-Martin, J. M., Dolmatova, E., Duffy, H. S. et al. (2011). Adult mouse epicardium modulates myocardial injury by secreting paracrine factors. *J. Clin. Invest.* **121**, 1894-1904.